A nozzle for high-density supersonic gas jets at elevated temperatures

C. M. Heyl, S. B. Schoun, G. Porat, H. Green, and J. Ye

View Online   Export Citation   CrossMark

Nanopositioning Systems

Modular Motion Control

AFM and NSOM Instruments

Single Molecule Microscopes

MCL
MAD CITY LABS INC.
www.madcitylabs.com

A nozzle for high-density supersonic gas jets at elevated temperatures

C. M. Heyl,[a)] S. B. Schoun, G. Porat, H. Green, and J. Ye

JILA, NIST and the University of Colorado, 440 UCB, Boulder, Colorado 80309-0440, USA

We present the development of a gas nozzle providing high-density gas at elevated temperatures inside a vacuum environment. Fused silica is used as the nozzle material to allow the placement of the nozzle tip in close proximity to an intense, high-power laser beam, while minimizing the risk of sputtering nozzle tip material into the vacuum chamber. Elevating the gas temperature increases the gas-jet forward velocity, allowing us to replenish the gas volume in the laser-gas interaction region between consecutive laser shots. The nozzle accommodates a 50 μm opening hole from which a supersonic gas jet emerges. Heater wires are used to bring the nozzle temperature up to 730 °C, while a cooling unit ensures that the nozzle mount and the glued nozzle-to-mount connection is kept at a temperature below 50 °C. The presented nozzle design is used for high-order harmonic generation in hot gases using gas backing pressures of up to 124 bars. © *2018 Author(s). All article content, except where otherwise noted, is licensed under a Creative Commons Attribution (CC BY) license (http://creativecommons.org/licenses/by/4.0/).* https://doi.org/10.1063/1.5051586

I. INTRODUCTION

The delivery of gases at controllable temperature, velocity, or density into a confined experimental target volume in a vacuum environment is a common task for various scientific or technological applications. This task is often accomplished using gas nozzles, optimized for various objectives. These include simple nozzles made of long and narrow capillaries and nozzles formed via a simple aperture separating a high pressure gas reservoir from the vacuum. While the first is easy to produce, the latter can provide high densities directly at the orifice. Other types, such as Laval nozzles[1] or pulsed Even-Lavie valves,[2,3] often complemented with skimmer arrangements, are optimized for minimum transverse beam velocities with maximized densities at large distances from the nozzle.[4] For different purposes, such as controlled cluster production[5] and/or in order to adjust the axial gas velocity, control of the gas temperature is important. Here we present a nozzle design optimized for multiple parameters: high gas density at the orifice, high gas temperature, and maximized axial gas velocity. The nozzle is designed for the application of high-order harmonic generation (HHG) in gases[6,7] with high-repetition rate (greater than 10 MHz) laser systems. For this application, ultra-short laser pulses are focused into a Xe gas jet emerging from the nozzle. Via HHG, the infrared laser pulses are converted into the extreme ultraviolet (XUV). A high gas density is required to maximize the nonlinear frequency conversion efficiency.[8] At the same time, the emerging gas needs to be confined to a small volume inside a vacuum chamber to avoid absorption of the ultraviolet radiation. A high gas axial speed is needed in order to avoid multiple interactions of the gas atoms with the high-repetition rate laser pulse train. This is achieved by mixing the Xe gas used for high-order harmonic generation

with a light carrier gas (He) and by heating the gas mixture.[9] In order to maximize the density in the laser-gas interaction volume, the laser focus is placed very close to the nozzle orifice. This sets high demands on the nozzle material as the laser average power is approximately 10 kW and intensities around 10^{14} W/cm^2 are reached in the laser focus.

II. NOZZLE DESIGN

Our nozzle design is based on a large outer diameter (8.57 mm) fused-silica capillary with large wall-thickness (inner diameter: 0.58 mm). Fused silica is a robust glass-material that allows the production of small inner-diameter capillaries and opening orifices by collapsing a larger-diameter capillary with a blowtorch. The large wall-thickness fulfills the extreme demands set on the material at high temperatures and large gas-pressure induced forces. Furthermore, it can be optically polished to reduce the interaction of the nozzle tip with intense laser fields. A schematic of the nozzle assembly is presented in Fig. 1.

The connection of the fused-silica capillary to a standard high-pressure gas line is realized via a brass socket (a modified NPT-type 3/8″ nut) into which the capillary is glued using a vacuum-compatible epoxy (Loctite Hysol 1C, also known as Torr Seal[3]). The epoxy is rated for temperatures up to 100 °C, making it necessary to keep the glued connection at low temperatures even when the upper part of the nozzle body is heated. This is achieved by enabling good heat transfer from the hot capillary to the water-cooled brass socket via a corrugated copper sheet. The corrugated copper provides high thermal conductivity and good surface contact area and allows for some deformation when the temperature changes.

In order to increase the gas temperature, the upper part of the nozzle capillary is heated via a heating wire. The wire is embedded into a ceramic layer, which keeps the heater wire in place while providing good heat transfer. In a first test version of this assembly, the ceramic layer was directly placed on

a)Also at Department of Physics, Lund University, P.O. Box 118, SE-221 00 Lund, Sweden. Now at Helmholtz-Institute Jena, Fröbelstieg 3, 07743 Jena, Germany and DESY, Notkestraße 85, 22607 Hamburg, Germany. Electronic mail: christoph.heyl@desy.de.

FIG. 1. Schematic of the nozzle assembly: The nozzle body, a thick-wall fused silica tube, is glued into a brass socket. Heater wires are wound around the nozzle body, held in place by ceramic. A graphite layer is added between the nozzle body and the ceramic to prevent direct ceramic-to-glass contact. A thermocouple (not shown) is embedded in ceramic between the graphite layer and the heating wire. A corrugated copper sheet allows heat transfer from the nozzle body to the water-cooled brass socket, ensuring a low temperature of the glued section of the nozzle. A stainless steel shield reduces heat radiation.

the fused silica capillary. However, due to a chemical reaction between the magnesium oxide ceramic and the silica occurring at high temperatures,[10] this direct contact has to be avoided. A graphite layer between the ceramic layer and the capillary solves this problem. For temperature monitoring, a thermocouple embedded in ceramic is placed between the graphite layer and the heating wire.

A stainless-steel heat shield surrounding the heated section of the nozzle reduces the radiative heat transfer to other objects placed close to the nozzle, transferring the heat to the water-cooled brass socket.

III. PRODUCTION PROCESS

A. The nozzle tip

The nozzle tip with an orifice diameter of 50 μm is produced using standard procedures for glass machining. While spinning the fused silica capillary around its central axis, a short section of the capillary is heated with a hydrogen torch. When the glass is fluid enough, the surface tension causes the capillary to collapse, leaving an inner diameter converging to zero. By collapsing the capillary without pulling, the length of the conical section of the nozzle can be minimized, leading to improved conductance and a small difference between backing pressure and actual pressure reached at the nozzle orifice. The collapsed capillary can be cut close to the onset of the nonzero inner diameter. By grinding the capillary starting at the cut surface, a well-defined orifice can be produced. For our application, where the nozzle tip needs to be placed very close to a laser focus, the abrasion surface is angled and polished to avoid beam blocking by the outer edges of the capillary and to reduce laser pulse-glass interaction. Figure 2 shows the nozzle tip.

After the glass machining steps are completed, all edges and surfaces are optically polished. As a last step, the nozzle

is uniformly baked to approximately 1215 °C to anneal the glass.

B. Mounting nozzle and heating assembly

The nozzle is squeezed into its brass mounting nut together with the flexible corrugated copper sheet. The latter is produced by forcing a thin copper foil through a suitable gear set and then hand-pinching into an accordion fold. The base of the nozzle is then glued into the brass socket using a vacuum-compatible low-vapor-pressure epoxy (Loctite Hysol 1C, also known as Torr Seal[3]). Afterwards, a pre-machined thin wall (1.2 mm thickness) graphite tube is slid over the nozzle. Care must be taken to match the inner diameter of the fragile graphite tube to the outer diameter of the nozzle. The graphite tube is then covered with a thin layer of quick-drying ceramic adhesive (Aremco Ceramabond 571[3]) onto which a thermocouple is placed, held in place by another ceramic layer. The heater wire (nichrome wire, gauge 32, i.e., 0.2 mm diameter)

FIG. 2. Optical microscope image of the nozzle tip body. The inset shows a magnified view of the orifice. Image colors are solely used to provide good visual contrast.

is then wound around the nozzle in two layers, separated by additional ceramic layers that hold the wire in place. In a last step, a stainless-steel tube is squeezed onto the upper part of the brass nut, leaving an air gap between the top ceramic layer and the heat shield. Thermocouple and heater wires can leave the nozzle through a slit in the heat shield.

IV. PERFORMANCE AND GAS MANAGEMENT

A. Gas management

The nozzle assembly is tested in air and in vacuum (10^{-6} mbar) at high, continuous backing pressures of up to 124 bars. Because of the high laser repetition rate, a pulsed gas jet design is not possible. At high backing pressures, a high gas load is reached in the vacuum chamber. In order to maintain a low pressure (in the presented case below 10^{-2} mbar), a two stage pumping system is used. First, as employed in earlier studies,[11,12] a gas-catch assembly is installed right in front of the nozzle opening (see Fig. 3). It consists of a conical cap with an opening hole of 1.5 mm diameter, connected to a large diameter pumping hose. A roughing pump (scroll pump) with a pumping speed of 110 l/min is connected to this hose. The gas-catch opening hole is placed at a distance of approximately 0.5 mm from the nozzle orifice. Second, the vacuum chamber (volume ≈ 0.175 m^3) is pumped by using a large turbo molecular pump (speed ≈ 1000 l/s).

B. Gas temperature

The nozzle was tested for outer-wall temperatures of up to 730 °C at a backing pressure of up to 124 bars. Long-term operation over several hours was performed at outer-wall temperatures of 560 °C. In order to avoid fast heat changes that may cause large internal material stress, the heating voltage was ramped up and down slowly, not exceeding a rate of 25 K/min.
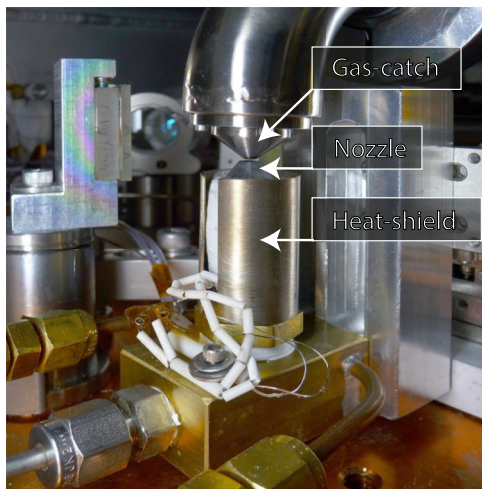
FIG. 3. Image of the nozzle assembly in the vacuum chamber as used for high-order harmonic generation in an optical enhancement cavity. The nozzle assembly is mounted on a 3D micro-positioning stage. The gas emerging through the nozzle hole passes a laser focus and is directed into a gas-catch assembly, consisting of a conical cap connected to a large diameter pumping hose (the bent steel tube visible at the top of the image) which is connected to a scroll pump.

While the nozzle temperature can be monitored easily, the gas temperature can be estimated using basic thermodynamic principles. For simplicity reasons, we assume that the outer surface of the glass nozzle has a uniform temperature. This is a good assumption as the glass is surrounded by a layer of graphite with much higher thermal conductivity than glass, equalizing the temperature along the heated section of the nozzle. We further assume that the outer glass surface temperature is equal to the temperature read by the thermocouple, independent of gas load. When operating the nozzle with high gas load (e.g., applying 80 bars of 9:1 He:Xe mixture), the thermocouple absolute temperature dropped by not more than 7% (e.g., from 830 K to approximately 770 K), justifying this assumption. The heat transfer rate $\dot{Q}$ through the wall of the cylindrical nozzle is given by[13]

$$\dot{Q} = -\frac{T_1 - T_2}{R_{cyl}}, \tag{1}$$

with T_1 and T_2 denoting the inner and outer wall temperatures of the glass nozzle, respectively. R_{cyl} denotes the thermal resistance of the nozzle glass cylinder. R_{cyl} can be calculated as $R_{cyl} = \frac{\ln(r_2/r_1)}{2\pi L k_{glass}}$ with r_1 and r_2 denoting the inner and outer nozzle surface radii, respectively, $L = 36$ mm is the length of the heated region of the nozzle, and k_{glass} is the temperature-dependent thermal conductivity of fused silica. Tabulated values for k_{glass} can easily be found in the literature, ranging from 1.38 W/(m K) at 20 °C to 2 W/(m K) at 550 °C. For simplicity reasons, we evaluate k_{glass} at the mean temperature $\overline{T}_{glass} = (T_1 + T_2)/2$. In steady-state conditions, conservation of energy requires the same heat conduction rate through the wall of the nozzle as through convection from the glass nozzle to the gas, which can be expressed as

$$\dot{Q} = \dot{m} c_p (T_e - T_i). \tag{2}$$

Here T_i and T_e denote the mean gas temperatures at the inlet and exit of the nozzle, respectively, $\dot{m}$ is the mass flow rate, and c_p is the specific heat capacity of the gas. Taking into account our nozzle geometry with the main gas flow limitation arising from the nozzle orifice area A_o, the mass flow rate for a supersonic gas jet can be expressed as a function of backing pressure P,[4]

$$\dot{m} = PA_o \sqrt{\frac{\gamma \overline{M}}{RT_e} \left(\frac{2}{\gamma + 1}\right)^{(\gamma+1)/(\gamma-1)}}, \tag{3}$$

where $\gamma = 1.66$ denotes the specific heat ratio for ideal monoatomic gases, R is the ideal gas constant, and $\overline{M} = X_1 M_1 + X_2 M_2$ denotes the molar average molecular mass of the gas mix with mole fraction X_i and mass M_i. The specific heat capacity can be calculated accordingly as[4] $c_p = [\gamma/(\gamma - 1)]R/\overline{M}$. Considering convective heat flow and neglecting radiative heat transfer, the exit temperature of a gas flowing through a pipe can be calculated. With the assumption that the nozzle inner surface temperature T_1 is approximately constant along the length of the heated section of the nozzle, justified by a small nozzle wall thickness compared to L, the mean gas exit temperature can be written as[13]

$$T_e = T_1 - (T_1 - T_i) \exp\left(-\frac{h A_s}{\dot{m} c_p}\right). \tag{4}$$

Here $A_s = \pi D L$ is the surface area of the inner wall of the nozzle with inner diameter D. The convection heat transfer coefficient h depends on various gas flow parameters including the type of convection, the flow geometry and shape, the flow motion (laminar or turbulent), the viscosity, and the compressibility as well as on gas density and temperature. For simplicity, we use the gas mean temperature $\overline{T}_{gas} = (T_i + T_e)/2$ to retrieve h. The heat transfer coefficient can be expressed as a function of the thermal conductivity of the gas and the so-called Nusselt number, describing the ratio of convective to conductive heat transfer. For a complete derivation of h, the reader is referred to the specialized literature.[13]

Setting Eqs. (1) and (2) equal to each other and inserting Eq. (4), we obtain an expression, which can be solved for the inner wall temperature, yielding

$$T_1 = T_i + \frac{T_2 - T_i}{1 + R_{cyl}\,\dot{m}\,c_p\left[1 - \exp\left(-\frac{h A_s}{\dot{m}\,c_p}\right)\right]}. \quad (5)$$

Using Eqs. (4) and (5), T_e can be calculated. However, as several temperature dependent quantities within these equations have to be evaluated using T_e and T_1, a numerical recursive approach has to be applied. The gas backing-pressure dependence enters via the mass flow rate. In addition, h is weakly pressure dependent.

The calculated gas temperature for pure Xe and He as well as for a 9:1 He:Xe gas mixture, as used for the application of high-order harmonic generation, is displayed in Fig. 4 as a function of gas pressure together with the corresponding nozzle inner-wall temperatures.

C. Application to high-order harmonic generation

As discussed in detail in a separate article,[9] the gas nozzle was implemented inside a passive optical enhancement resonator for HHG in a gas jet. The employed laser parameters are a central wavelength of 1070 nm, pulse duration of 130 fs, repetition rate of 77 MHz, and intra-cavity laser average power of 10-15 kW. HHG always involves some ionization of the
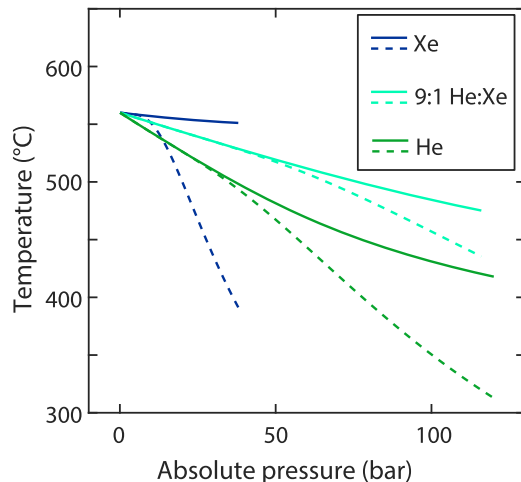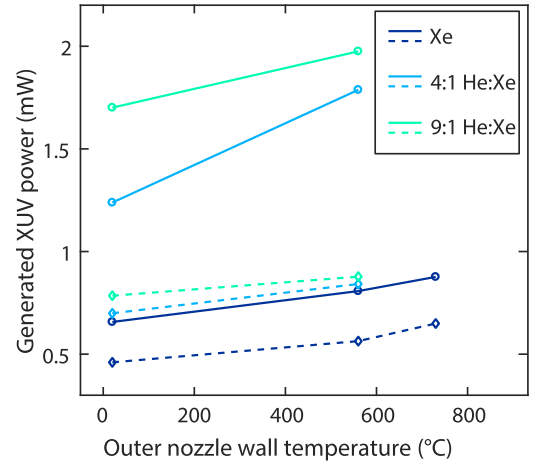

FIG. 5. Generated XUV power at 97 nm (solid lines and circles) and 63 nm (dashed lines and diamonds) measured at a few sample outer nozzle wall temperatures T_2 for different gas mixtures. For each data point, the XUV power is optimized by adjusting the gas pressure.

gas. Operating at repetition rates above a few MHz leads to the accumulation of free electrons inside the gas jet as each atom interacts with more than one laser pulse. In our experimental geometry, taking into account an estimated diameter of the effective interaction volume $w_{eff} \approx 18\ \mu m$ at 41 μm laser focal spot diameter (FWHM) and a Xe supersonic jet velocity of 310 m/s at room temperature, at least 4 laser pulses interact with each atom. As high ionization levels limit the HHG average power, phase-matched operation is no longer possible above a critical ionization level[9] due to the plasma contribution to the optical dispersion. By increasing the gas jet forward velocity, this problem can be avoided. This was achieved by (i) mixing the heavy Xe gas used for HHG with light helium gas and (ii) by heating up the gas jet. Figure 5 displays the maximum generated XUV average power for harmonic 11 (97 nm) and harmonic 17 (63 nm) as a function of nozzle outer wall temperature for different gas mixture ratios. While the main power increase is reached by changing from pure Xe to the 9:1 He:Xe mixture (requiring ~10× higher backing pressure of up to ~90 bars), the power is improved further with temperature for all gas mixtures, owing to the gas velocity v_{gas} increasing as

FIG. 4. Calculated gas temperature T_e (dashed) and inner wall nozzle temperature T_1 (solid) as a function of gas pressure for different gases, assuming $T_2 = 560\ °C$.

TABLE I. Optimum absolute gas backing pressures and gas velocities for different He:Xe gas mixtures and temperatures corresponding to the data presented in Fig. 5.

Mix	T_2 (°C)	Harmonic 11		Harmonic 17	
		v_{gas} (m/s)	P_{opt} (bar)	v_{gas} (m/s)	P_{opt} (bars)
Xe	20	305	5.0	305	5.7
	560	512	7.7	512	7.7
	730	563	5.0	563	7.7
4:1	20	643	11	643	15
	560	1068	39	1060	56
9:1	20	853	25	853	35
	560	1382	70	1363	87

$v_{\text{gas}} \propto \sqrt{T_e}$.[4] The displayed data can be seen as lower bounds of the generated average power as the XUV power was measured after diffraction from an XUV grating, followed by reflection at a gold mirror. For diffraction and reflection, the theoretically optimum values were taken into account, neglecting losses due to mirror and grating imperfections, resulting in an underestimated average XUV power. Measured optimum absolute gas backing pressures P_{opt} and calculated gas velocities v_{gas} corresponding to the data presented in Fig. 5 are displayed in Table I.

V. PUSHING THE DESIGN LIMITS: HIGHER GAS DENSITIES AND HIGHER TEMPERATURES

The current nozzle design is optimized for high-density gas operation, allowing one to heat the gas under continuous operation up to $\approx 550\,^\circ$C, depending on gas mixture and backing pressure. The maximum temperature is limited mainly by the heating power which can be transferred into the system, restricted by the damage threshold of the heating wires. Note that this damage threshold is different for the operation in vacuum and in air as higher wire temperatures are reached for the same current in vacuum due to the absence of convective cooling. In the present design, a large fraction of the heating power is directly transferred from the heating wires via the thermally conductive graphite tube to the cooled brass socket. To lower this heat loss and thus improve the heat transfer to the nozzle, a gap between the lower end of the graphite tube and the brass socket could be added. Additionally, larger-diameter nichrome wires could support a higher heating power, albeit requiring longer wires or higher electrical current. The ultimate temperature limit is set by the material properties of the fused silica with a melting point around 1650 $^\circ$C. However, already temperatures approaching the annealing point (around 1170 $^\circ$C), where the nozzle body can start to deform, will likely set a limit. Better heat transfer into the gas could also be achieved by extending the length of the heated section of the nozzle. In the presented design, this length is limited by space restrictions for the total length of the assembly.

The system was tested for a maximum backing pressure of 124 bars, limited in the presented case by the pressure rating of the gas supply tubing and the gas bottle filling pressure. The nozzle assembly can likely take higher pressures.

VI. CONCLUSION

We have demonstrated a high-temperature glass nozzle capable of delivering a high-density supersonic gas jet close to the focus of a high-power laser beam. The nozzle can simultaneously handle temperatures of 730 $^\circ$C and backing pressures of 124 bars. Continuous operation of this nozzle over many hours inside a delicate optical resonator placed in a vacuum environment was demonstrated, enabling the generation of coherent radiation at 12.7 eV with record average power around 2 mW.[9]

ACKNOWLEDGMENTS

[1] J. Lee and G. Stein, J. Phys. Chem. **91**, 2450 (1987).
[2] U. Even, Adv. Chem. **2014**, 636042.
[3] The description of the product name is for the sole purpose of technical communication, and it does not represent an official endorsement by NIST (2005).
[4] G. Scoles, *Atomic and Molecular Beam Methods* (Oxford University Press, 1988).
[5] O. F. Hagena and W. Obert, J. Chem. Phys. **56**, 1793 (1972).
[6] A. McPherson, G. Gibson, H. Jara, U. Johann, T. S. Luk, I. A. McIntyre, K. Boyer, and C. K. Rhodes, J. Opt. Soc. Am. B **4**, 595 (1987).
[7] M. Ferray, A. L'Huillier, X. F. Li, L. A. Lompré, G. Mainfray, and C. Manus, J. Phys. B: At. Mol. Opt. Phys. **21**, L31 (1988).
[8] C. Heyl, C. Arnold, A. Couairon, and A. L'Huillier, J. Phys. B: At. Mol. Opt. Phys. **50**, 013001 (2017).
[9] G. Porat, C. M. Heyl, S. B. Schoun, C. Benko, N. Dörre, K. L. Corwin, and J. Ye, Nat. Photonics **12**, 387 (2018).
[10] S. Mikhail and P. King, J. Therm. Anal. **40**, 79 (1993).
[11] D. Yost, "Development of an extreme ultraviolet frequency comb for precision spectroscopy," Ph.D. thesis, University of Colorado, 2005.
[12] C. Guo, A. Harth, S. Carlström, Y.-C. Cheng, S. Mikaelsson, E. Mårsell, C. M. Heyl, M. Miranda, M. Gisselbrecht, M. B. Gaarde, K. J. Schafer, A. Mikkelsen, J. Mauritsson, C. L. Arnold, and A. L'Huillier, J. Phys. B: At. Mol. Opt. Phys. **51**, 034006 (2018).
[13] Y. A. Çengel and A. J. Ghajar, *Heat and Mass Transfer: Fundamentals and Applications*, 4th ed. (McGraw-Hill, 2011).